Published in final edited form as:
J Mol Biol. 2008 May 30; 379(2): 331–342.

Crystal Structure of the MACPF Domain of Human Complement Protein C8α in Complex with the C8γ Subunit

Daniel J. Slade[1], **Leslie L. Lovelace**[1], **Maksymilian Chruszcz**[2], **Wladek Minor**[2], **Lukasz Lebioda**[1], and **James M. Sodetz**[1]

1*Department of Chemistry and Biochemistry, University of South Carolina, Columbia, SC 29208*

2*Department of Molecular Physiology and Biological Physics, University of Virginia, Charlottesville, VA 22908*

Summary

Human C8 is one of five complement components (C5b, C6, C7, C8 and C9) that assemble on bacterial membranes to form a pore-like structure referred to as the "membrane attack complex" (MAC). C8 contains three genetically distinct subunits (C8α, C8β, Cγ.) arranged as a disulfide-linked C8α-γ dimer that is noncovalently associated with C8β. C6, C7 C8α, C8β and C9 are homologous. All contain N- and C-terminal modules and an intervening 40-kDa segment referred to as the membrane attack complex/perforin (MACPF) domain. The C8γ subunit is unrelated and belongs to the lipocalin family of proteins that display a β-barrel fold and generally bind small, hydrophobic ligands. Several hundred proteins with MACPF domains have been identified based on sequence similarity; however, the structure and function of most are unknown. Crystal structures of the secreted bacterial protein Plu-MACPF and the human C8α MACPF domain were recently reported and both display a fold similar to the bacterial pore-forming cholesterol-dependent cytolysins (CDC). In the present study, we determined the crystal structure of the human C8α MACPF domain disulfide-linked to C8γ (αMACPF-γ) at 2.15 Å resolution. The αMACPF portion has the predicted CDC-like fold and shows two regions of interaction with C8γ. One is in a previously characterized 19-residue insertion (indel) in C8α and fills the entrance to the putative C8γ ligand binding site. The second is a hydrophobic pocket that makes contact with residues on the side of the C8γ β-barrel. The latter interaction induces conformational changes in αMACPF that are likely important for C8 function. Also observed is structural conservation of the MACPF signature motif Y/W-G-T/S-H-F/Y-X_6-G-G in αMACPF and Plu-MACPF, and conservation of several key glycine residues known to be important for refolding and pore formation by CDCs.

Keywords

complement; MACPF; C8; cytolysins; membrane attack complex

Corresponding authors: J.M.S. (sodetz@mail.chem.sc.edu); L.L. (lebioda@mail.chem.sc.edu).

Accession code - Protein Data Bank: αMACPF-γ atomic coordinates together with structure factors have been deposited with accession code **2RD7**.

Introduction

Assembly of the complement membrane attack complex (MAC) on the surface of gram-negative bacteria and other pathogenic organisms involves the sequential interaction of complement proteins C5b, C6, C7, C8 and C9 and formation of a transmembrane pore composed of multiple C9 molecules.[1–3] The sequence of interactions leading to MAC formation is well defined; however, the mechanism by which the MAC disrupts membrane organization is poorly understood. MAC assembly begins with local production of C5b by activated complement and binding of C6 to form a soluble, noncovalently-linked C5b-6 complex. Subsequent binding of C7 produces a complex (C5b-7) with an affinity for cell membranes. C5b-7 binds to the outer portion of membrane bilayers and only minimally penetrates the interior.[4] Once on the membrane, C5b-7 binds C8 and forms a tetrameric C5b-8 complex. The ultrastructure of C5b-8 has no pore-like features; however, this complex causes leakage of synthetic lipid vesicles,[5] increases ion-conductance in planar lipid bilayers,[6] and promotes the slow osmotic lysis of simple cells such as heterologous erythrocytes.[7] Photolabeling studies using extracellular or membrane-restricted probes identified the C8α subunit as the major C5b-8 component inserted in the membrane.[8,9] In the final step of MAC formation, C5b-8 binds and initiates the self-polymerization of C9 to form a cylindrical transmembrane pore composed of 12–18 C9 molecules.[3,10]

C8 has the most complex subunit arrangement of the five MAC components. It contains three genetically distinct proteins (C8α, C8β, C8γ) arranged as a disulfide-linked C8α-γ heterodimer that is noncovalently associated with C8β.[11,12] C8α and C8β are homologous to each other and to C6, C7 and C9. These five proteins comprise the "MAC family" of proteins; all contain a variable number of N- and C-terminal modules and a central 40-kDa MACPF domain.[13,14] The MACPF domain was named as such because it is conserved in the MAC family proteins and perforin. The 20-kDa C8γ subunit is unrelated to the other MAC proteins and has the distinction of being the only lipocalin in the complement system.[15]

Several hundred proteins have been identified as having MACPF domains. They exhibit limited sequence similarity but contain a signature Y/W-G-T/S-H-F/Y-X_6-G-G MACPF motif.[16] With a few exceptions, such as the MAC proteins and perforin which are known to form lytic pores for immune defense,[17] the function of most MACPF proteins is unknown. Crystal structures of two MACPF proteins were recently published concurrently by two different groups. Plu-MACPF from the gram-negative bacteria *Photorhabdus luminescens* was found to display a fold similar to the bacterial pore-forming cholesterol-dependent cytolysins (CDC).[18] Although nonlytic, Plu-MACPF was shown to bind to cell membranes. The second protein was the MACPF domain from human C8α, which studies showed could be produced recombinantly and in a functional form.[19] The crystal structure of this protein (C8α-MACPF) was solved and also found to display a CDC-like fold.[20] Pore-formation by CDCs occurs by self-polymerization of 30–50 monomers on target membrane surfaces, followed by a major refolding, and insertion of transmembrane β-hairpins (TMH).[21] Structural similarity between C8α-MACPF and the CDCs suggests that complement MAC proteins use a CDC-like mechanism for pore formation.

In addition to the human C8α MACPF domain, we recently described the production of a disulfide-linked heterodimer (αMACPF-γ) composed of the C8α MACPF domain (αMACPF) and C8γ.[19] Correct folding of αMACPF-γ was inferred from its ability to bind C8β and C9 and form a functional MAC. We now report the crystal structure of αMACPF-γ as determined by X-ray diffraction. A comparison to the previously reported C8α-MACPF structure reveals conformational differences in αMACPF that are induced by C8γ, and may be important for C8 function. Also described are conserved features in the C8α MACPF domain and Plu-MACPF that were not compared previously because the structures were published concurrently. Our

analysis shows structural conservation of the signature Y/W-G-T/S-H-F/Y-X_6-G-G motif in αMACPF and Plu-MACPF as well as conservation of several key glycine residues known to be important for CDC refolding and pore formation.

Results

Structure of αMACPF-γ

The crystal structure of αMACPF-γ was determined to 2.15 Å resolution (Table 1 and Fig. 1a). Both intrachain disulfide bonds in αMACPF (C8α C110-C147 and C345-C369) and the single interchain disulfide bond between αMACPF C164 and C8γ C40 are correctly formed. The extension of C8γ to one side makes αMACPF-γ an unusually thin and wide globular protein (70Å tall, 80Å wide, and 20Å thick) (Fig. 1b). In agreement with the C8α-MACPF structure, the central feature of αMACPF is an L-shaped four-stranded antiparallel β-sheet that is flanked by two groups of α-helices. Secondary Structure Matching (SSM)[22] software identified the overall structural similarity between the αMACPF portion and the CDCs intermedilysin (ILY) from *Streptococcus intermedius*[23] and perfringolysin O (PFO) from *Clostridium perfringens*.[24]

αMACPF is a single domain protein that contains regions corresponding to what are referred to as domains 1 and 3 in ILY (Fig. 1d). Domain 3 in ILY contains two small α-helical bundles referred to as TMH1 and TMH2 because of their ability to unfold and form transmembrane β-hairpins during CDC pore formation. For the sake of clarity, we have used the ILY terminology to identify corresponding regions in αMACPF. αMACPF-γ lacks the flexible linker domain 2 and the membrane-interacting, Ig-like β-sandwich domain 4 in ILY. Domain 4 in ILY and C8γ in αMACPF-γ both extend outward but in radically different locations with respect to the core β-sheet. Also, TMH1 in αMACPF is longer than in ILY and forms two additional hydrophobic, antiparallel β-strands (β-strands 5 and 6) that hydrogen bond to the main β-sheet and extend it to six strands at the top. As observed with C8α-MACPF, the disulfide loop formed by C345-C369 in TMH2 is disordered in αMACPF-γ. This loop lies within the segment of C8α that contains the binding site for CD59, a complement regulatory protein that inhibits MAC formation by binding to C8α and C9.[25,26]

A sample of electron density shows the core β-sheet portion of αMACPF is well defined (Fig. 2). Several other segments show considerable flexibility as judged by less-defined density. A model could not be built for αMACPF residues 103–109, 355–366, 371–373, and 396–409 although some discontinuous electron density for these regions is present.

The structure of C8γ within αMACPF-γ agrees well with the structure determined for C8γ alone.[27] C8γ is a member of the lipocalin family of proteins that display a β-barrel fold that forms a calyx with a binding pocket for a small, generally hydrophobic ligand.[28] Although it has a lipocalin fold, the existence of a natural small-molecule ligand for C8γ has not been established. In C8α, the binding site for C8γ lies within a 19-residue insertion (indel) in the MACPF domain and contains C8α C164 that covalently links to C8γ C40.[29] Crystallographic studies of C8γ in complex with a synthetic C8α indel peptide showed that the indel residues make contacts with all four loops at the opening of the calyx and completely fills the entrance.[30] The αMACPF-γ structure is in complete agreement with these findings. The indel segment of αMACPF forms a two-stranded β-sheet at the end of an extension of mostly charged residues and interacts with all four loops at the entrance to the C8γ calyx. The calyx entrance is completely filled and the loops are moved even closer to the indel in αMACPF than in the C8γ-indel peptide complex (Fig. 3). Loop 1 is moved substantially, perhaps because of the disulfide bond between C8γ C40 in loop 1 and C8α C164 in αMACPF. In the C8γ-indel peptide complex, these residues are substituted with alanine.

αMACPF-γ and C8α-MACPF structure comparison

A comparison performed by SSM shows that αMACPF-γ and C8α-MACPF contain 249 residues that align well to give a RMSD of 2.1Å (Fig. 4a). Major differences lie in the TMH1 segment and in regions that interact with C8γ. In C8α-MACPF, TMH1 begins with helix B, and then takes a sharp turn into a newly formed helix B' (Fig 4b). Helix B' is bent 90° away from helix B and proceeds into β-strand 6. β-strand 6 connects to the anti-parallel β-strand 5 and then down into helix C. In this conformation, β-strand 6 interacts with β-strand 4 in the core β-sheet. This arrangement is the reverse of what is seen in the αMACPF-γ structure, where TMH1 begins with a straight helix B and leads directly into γ-strand 6 (Fig. 4c). β-strand 6 then leads to the antiparallel β-strand 5 and down into helix C. The structure is much more vertical, with no bend in helix B and no disruption in bonding between β-strands 4, 5, and 6 in the core β-sheet. These differences appear to be related to contacts in the C8α-MACPF structure between residues 213–215 of helix B′ with symmetry equivalent residues of a neighboring molecule in the crystal. This region has well defined electron density in both structures, thus the differences are not a result of alternate interpretations by the authors. The ability of crystal contacts to alter the conformation suggests flexibility in the TMH1 region, which could facilitate refolding during membrane insertion of C8α.

In addition to the C8α indel, C8γ binds to a second region of αMACPF. F174 from C8γ fits in a hydrophobic pocket created by αMACPF residues L190 (β-strand 1), V266 (β-strand 2), and Y413 (I-helix) (Fig 5a). This pocket is not present in the C8α-MACPF structure.

Superposition of this region of C8α-MACPF on αMACPF-γ shows that L190 and Y413 in αMACPF have altered their conformation to facilitate interaction with C8γ F174 (Fig. 5b). Movement of L190 causes β-strand 1 of αMACPF to move closer to C8γ. Importantly, movement of Y413 in αMACPF also causes the I-helix to move closer to C8γ and pull away from β-strand 4. In CDCs, movement of the I-helix during pore formation provides access to β-strand 4 and allows for edge sharing with β-strand 1 from a neighboring monomer.[31] C8γ may facilitate a similar interaction between β-strands in C8α and those in the neighboring MAC components. Such a possibility could explain why MAC formed with a C8 analogue composed of only C8α + C8β is much less lytically active than MAC formed with intact C8.[32,33]

Comparison of αMACPF-γ to CDCs and Plu-MACPF

An analysis performed by SSM shows that αMACPF-γ and ILY contain 149 residues within domains 1 and 3 that superimpose well and give a RMSD of 4.7 Å (Fig. 6). A superposition and SSM structure comparison of αMACPF-γ and Plu-MACPF likewise shows similar folds for domains 1 and 3 with 192 residues that superimpose well with a RMSD of 3.9 Å. These superpositions clearly show that relative to the core β-sheet, C8γ is in a completely different position from domain 4 in ILY and the β-prism domain in Plu-MACPF.

Superposition of αMACPF-γ on Plu-MACPF shows the MACPF domain signature motif Y/W-G-T/S-H-F/Y-X_6-G-G is structurally conserved (Fig. 7). The first five residues (Y/W-G-T/S-H-F/Y) lie in a region that corresponds to the interface between domains 1 and 3 in CDCs. αMACPF contains the sequence YGTHY (residues 307–311), while Plu-MACPF contains WGSHF (residues 198–202). Internal contacts within this motif are made between T309 with H310 in αMACPF and S200 with H201 in Plu-MACPF. Although the fold of domains 1 and 3 in ILY and PFO are similar to corresponding regions of Plu-MACPF and αMACPF, the MACPF sequence motif is not conserved in CDCs.

The two glycines at the end of the MACPF motif in αMACPF (G318, G319) and Plu-MACPF (G209, G210) extend into the middle of β-strand 3. Although the entire MACPF motif is not conserved in CDCs, the location of these glycines correspond approximately to G301 in ILY

and G274 in PFO. These may provide flexibility in the core β-sheet of MACPF proteins, as is thought to be the case with the CDCs.[24] A second pair of conserved glycines in αMACPF (G395, G396) and Plu-MACPF (G270, G271) are in the same structural location as G351 and G352 in ILY, and G324 and G325 in PFO. In ILY and PFO, these glycines lie at the junction between β-strand 4 and 5. They allow β-strand 5 and the I-helix to swing away from β-strand 4 of the core β-sheet,[31] which permits β-strand 4 to edge-share and hydrogen bond with β-strand 1 of a neighboring CDC molecule during pore formation. The conserved location suggests these glycines could function similarly in the MACPF proteins.

Comparison of TMH sequences within the MAC family proteins

The two α-helical bundles at the base of the core β-sheet in ILY and PFO contain 30–35 residues, and when completely unfolded are of sufficient length to form a transmembrane β-hairpin. This was shown for PFO where the TMH segments have 23–28 residues inserted in the membrane in a fully assembled pore.[34,35] TMH1 and TMH2 in αMACPF are much longer with 56 and 57 residues, respectively. Whether a portion of each forms β-hairpins comparable in length to the CDCs or if each unfolds to form longer β-hairpins cannot be predicted. A comparison of the αMACPF TMH1 and TMH2 sequences to corresponding regions in the MAC family proteins reveals several interesting features (Fig. 8). The segments are all much longer than corresponding regions in the CDCs. In C6 and C7, the TMH1 segments are largely hydrophilic, which suggests membrane penetration by this region would be limited. This is in contrast to the central portions of TMH1 in C8α and C8β, which are rich in hydrophobic residues. In C9, the most striking feature of TMH1 is its length, which is extended to 74 residues because of an insertion. If the C9 MACPF structure is similar to αMACPF, such an insertion would result in a greatly extended region between β-strands 5 and 6. As suggested by others,[20] the length and alternating pattern of hydrophobic and hydrophilic residues makes it likely this region of C9 forms transmembrane β-hairpins as C9 undergoes self-polymerization to form the MAC pore.

A comparison of TMH2 sequences shows conservation of cysteines that form the disulfide loop in TMH2 of αMACPF (C345–C369). Corresponding loop segments in C6 and C7 are more hydrophilic and much shorter than in C8α, C8β and C9. In the latter proteins, the disulfide loops contain a greater percentage of hydrophobic residues along with charged residues in the center that may facilitate initial contact with the membrane.

Discussion

Until recently there was limited structural information available for the MAC proteins. Solving the human C8α-MACPF structure and revealing its similarity to the CDCs was a major advancement as it provided mechanistic insight into how the MAC forms pores. This structure and its similarity to the bacterial Plu-MACPF structure showed that the CDC-like fold is conserved in MACPF proteins from distant organisms. The present study extends these findings by providing additional structural information on C8 and insight into how C8γ may influence C8 function. Features in αMACPF and Plu-MACPF that were not compared in earlier studies have also been further analyzed.

The αMACPF-γ structure shows that the entrance to putative ligand binding pocket in C8γ is completely filled by the C8α indel. This agrees with previous conclusions based on studies using the C8α indel peptide. One distinctive feature of C8γ compared to most lipocalins is the division of its ligand binding pocket into a hydrophilic upper portion and a large hydrophobic lower cavity. Access to the latter is restricted by the close proximity of two tyrosine side chains; however its been shown using lauric acid as a pseudoligand that penetration into the lower cavity occurs if a ligand is narrow and hydrophobic at one end.[36] Interestingly, the αMACPF-γ structure shows no ligand trapped in the lower cavity. This observation and complete

occupancy of the upper cavity by the indel further supports the likelihood that a small-molecule ligand is not normally bound to C8γ within C8. If such a natural ligand exists, binding would require a major conformational change to expose the C8γ binding pocket as C8 incorporates into the MAC.

The αMACPF-γ structure also shows that C8γ makes contact with β-strands 1 and 2, and the I-helix in αMACPF. This significantly alters the local αMACPF conformation and may explain the strong positive affect C8γ has on C8 activity. Several studies have shown that MAC formed with C8 composed of C8α + C8γ has only ~ 15% of the hemolytic and bactericidal activity of MAC formed with intact C8.[32,33] The mechanism by which C8γ increases C8 activity is unknown. Photolabeling and binding studies suggest C8γ is located on the periphery of the MAC and does not enhance activity by direct penetration into the membrane.[9,37] One possibility is the altered position of β-strand 1 or the I-helix in the presence of C8γ may facilitate unfolding of C8α to allow edge-sharing and more efficient MAC formation. Another possibility is that the conformational change induced by C8γ may affect the C9 binding site, which lies within the C8α MACPF domain.[19] C8γ may simply increase the binding affinity for C9 and enhance formation of a fully functional MAC.

C8γ extends out from the core β-sheet of αMACPF much like the Ig-like β-sandwich domain 4 in PFO and ILY, and the β-prism domain in Plu-MACPF. These domains contain anti-parallel β-strands connected by loops at the top and bottom. Mutagenesis studies of domain 4 in PFO showed that residues within the four loops at the bottom are necessary for membrane binding and pore formation.[38] The β-prism domain of Plu-MACPF has a fold similar to domain 4 of CDCs. The function of this domain in Plu-MACPF is unknown, however a similar β-sandwich domain in the protein equinatoxin from the actinoporin pore-forming protein family was shown to directly facilitate membrane binding to phosphorylcholine molecules through its lower loops.[39] Another structurally similar β-prism domain in *Vibrio cholerae* cytolysin contains a carbohydrate binding site,[40,41] and removal of this domain results in a significant loss of hemolytic activity. C8γ has a lipocalin β-barrel fold and like the above domains contains anti-parallel β-strands connected by loops at the top and bottom. This raises the interesting question of whether C8γ might enhance MAC lytic activity by interacting with unidentified molecules on the membrane surface, possibly through its bottom loops or other accessible regions such as its α-helix.

CDC pore formation is initiated by edge-on hydrogen bonding between strands of the core β-sheets from neighboring monomers as they assemble on target membranes. Once a circular pre-pore is formed, domain 3 helical bundles in each monomer refold to form aligned amphipathic TMHs, which insert and form the β-barrel pore.[42] Assembly of a functional MAC pore is more complex because it involves the sequential interaction of five different components composed of seven different proteins. Because they are homologous and have conserved MACPF domains, one can predict that C6, C7, C8β and C9 will have core structural features similar to αMACPF. Although there is no evidence for pore-formation by C5b-8, similar structures for the other MACPF domains would suggest that unfolding of TMH helices and at least partial insertion of β-hairpins is the primary mechanism by which C5b-8 is anchored to membranes.

A mechanism for MAC formation based on edge-sharing and hydrogen bonding between β-hairpins of MACPF domains would be consistent with what is known about MAC protein interactions. C5b-6 contains only one MACPF component (C6) and is a soluble complex with no affinity for membranes. Addition of C7 to form C5b-7 induces a conformational change that facilitates binding to membranes. Binding between C6 and C7 may promote unfolding and partial insertion of their respective TMH segments. Alignment of neighboring β-hairpins in a C6–C7 manner may be crucial for formation of a stable complex and lowering the energy

barrier for partial insertion. Since the predicted TMH sequences in C6 and C7, and the TMH2s in particular, are shorter and more hydrophilic than in C8α, C8β or C9, the C5b-7 complex may become anchored but with minimal membrane penetration and disruption.

Studies using model membranes and cell systems have shown that significant membrane disruption first occurs with formation of C5b-8. Within C8, the C8β subunit contains two distinct binding sites, one that binds C5b-7 and one that binds C8α. Importantly, both reside within the MACPF domain of C8β.[43] C8α also has two distinct binding sites, one for C8β and one for C9. Both of these sites lie within the MACPF domain of C8α.[19] The fact that key binding sites lie within the MACPF domains in both C8α and C8β supports a CDC-like mechanism of edge-sharing and β-hairpin formation. Upon binding of C8 to C5b-7, interaction between C8β and either C6 or C7 could induce unfolding of TMHs in C8β, and subsequently those in C8α to form an extended series of aligned β-hairpins. TMHs in C8α and those predicted for C8β are longer and more hydrophobic than those in C6 and C7, which may explain the increase in membrane disruption when C8 binds to C5b-7. Alignment of several β-hairpins could create a more energetically favorable arrangement for deeper membrane insertion. This zippering effect of adding the next molecule, unfolding its TMH segments and forming hydrogen bonds between adjoining β-hairpins, occurs during CDC pre-pore formation. The C9 binding site lies within αMACPF, thus unfolding of αMACPF TMHs in C5b-8 could allow edge-sharing with C9. Subsequent edge-sharing between C9 molecules could then lead to self-polymerization of C9 and pore formation.

The MAC family proteins and perforin are known to participate in lytic pore formation. Only a few other MACPF proteins have been characterized and several are also thought to form pores for invasion or protection. Examples are proteins from malarial parasites,[44] the cytolytic toxins from sea anemones,[45] and proteins that provide plant immunity.[46] We have shown that several glycines considered important for CDC pore formation map to the same structural location in αMACPF and Plu-MACPF, and therefore are likely to be important for the function of MACPF proteins that form pores. As described by others,[18] two of these glycines in Plu-MACPF (G270, G271) align based on sequence analysis with G305 and G306 in perforin. Genetic mutations in these residues in perforin have been linked to disease.[47] Interestingly, one of the more common causes of human complement C7 deficiency is linked to residue G357 in the C7 MACPF domain.[48] This residue corresponds to G395 in αMACPF and G270 in Plu-MACPF, which are among the conserved glycines considered functionally important in CDCs. Our analysis also shows that the MACPF signature motif Y/W-G-T/S-H-F/Y-X_6-G-G is structurally conserved in αMACPF and Plu-MACPF. The significance of this motif is presently unclear, however evolutionary conservation between humans and bacteria suggests a functional role. The precise nature of that role must await the characterization of additional MACPF domain proteins.

Methods

Protein expression and crystallization

Human αMACPF containing C8α residues 103–462 was co-expressed with C8γ in *Escherichia coli*, purified, and characterized as described elsewhere.[19] Initial crystallization conditions of αMACPF-γ were identified by the high-throughput screening facility at Hauptman-Woodward Medical Research Institute, Inc. (Buffalo, NY).[49] To assist with structure solving, SeMet αMACPF-γ was produced using the M9 SeMET High-Yield Growth Media Kit Package (Medicilon, Inc.). Purified αMACPF-γ and SeMet αMACPF-γ were concentrated to 5 mg mL^{-1} in 0.05 M Tris, 0.15 M NaCl, pH 8.0, and crystallized at 16 °C by hanging drop vapor diffusion in 6% (w/v) PEG 20,000, 0.1 M citric acid, 0.025 M $Mg(NO_3)_2$, pH 5.0. Crystals were incubated in 80% (v/v) crystallization solution + 20 % (v/v) MPD and flash frozen in a stream of nitrogen vapor at 100K.

Structure determination and refinement

Data from a SeMet αMACPF-γ crystal were collected at 100K on beamline 19-ID of the Structural Biology Center at the Advanced Photon Source, Argonne National Laboratory, and processed with *HKL-2000*.[50] The structure was solved and the initial model built using anomalous diffraction from single wavelength data with *HKL-3000*,[51] which is integrated with *SHELXD*,[52] *SHELXE*,[53] *MLPHARE*,[54] *DM*,[55] *O*,[56] *COOT*,[57] *REFMAC5*,[58] *ARP/wARP*,[59] and *RESOLVE*.[60] The initial model was extended by a combination of manual rebuilding with *COOT* and automatic model rebuilding with *ARP/wARP* and *RESOLVE*. *REFMAC5* was used to refine the model against higher-resolution native αMACPF-γ data collected on SER-CAT beamline 22-ID at Argonne National Laboratory. Structure superpositions were created using DaliLite.[61] Ribbon representations in Fig. 1 were generated using Molscript/Raster3D.[62,63] Unless specified, other figures were produced using PyMOL.[64]

Acknowledgments

We are grateful for the assistance of the high-throughput crystallization laboratory at Hauptman-Woodward Medical Research Institute, Inc., Buffalo, NY., and the staff at SBC and SER-CAT beamlines at APS. Use of APS was supported by the U. S. Department of Energy, Office of Basic Energy Sciences, under Contract W-31-109-Eng-38. This research was supported by NIH Grants GM042898 to J.M.S. and GM053163 to W.M.

References

1. Müller-Eberhard HJ. Molecular organization and function of the complement system. Annu. Rev. Biochem 1988;57:321–347. [PubMed: 3052276]
2. Esser AF. The membrane attack complex of complement. Assembly, structure and cytotoxic activity. Toxicology 1994;87:229–247. [PubMed: 8160186]
3. DiScipio RG, Berlin C. The architectural transition of human complement component C9 to poly(C9). Mol. Immunol 1999;36:575–585. [PubMed: 10499811]
4. Esser AF, Kolb WP, Podack ER, Müller-Eberhard HJ. Molecular reorganization of lipid bilayers by complement: a possible mechanism for membranolysis. Proc. Natl. Acad. Sci. U.S.A 1979;76:1410–1414. [PubMed: 220614]
5. Zalman LS, Müller-Eberhard HJ. Comparison of channels formed by poly C9, C5b-8 and the membrane attack complex of complement. Mol. Immunol 1990;27:533–537. [PubMed: 1696352]
6. Shiver JW, Dankert JR, Esser AF. Formation of ion-conducting channels by the membrane attack complex proteins of complement. Biophys. J 1991;60:761–769. [PubMed: 1720679]
7. Ramm LE, Whitlow MB, Mayer MM. Size of the transmembrane channels produced by complement proteins C5b-8. J. Immunol 1982;129:1143–1146. [PubMed: 6286757]
8. Podack ER, Stoffel W, Esser AF, Müller-Eberhard HJ. Membrane attack complex of complement: distribution of subunits between the hydrocarbon phase of target membranes and water. Proc. Natl. Acad. Sci. U.S.A 1981;78:4544–4548. [PubMed: 6270682]
9. Steckel EW, Welbaum BE, Sodetz JM. Evidence of direct insertion of terminal complement proteins into cell membrane bilayers during cytolysis. Labeling by a photosensitive membrane probe reveals a major role for the eighth and ninth components. J. Biol. Chem 1983;258:4318–4324. [PubMed: 6833260]
10. DiScipio RG. The relationship between polymerization of complement component C9 and membrane channel formation. J. Immunol 1991;147:4239–4247. [PubMed: 1721643]
11. Ng SC, Rao AG, Howard OM, Sodetz JM. The eighth component of human complement: evidence that it is an oligomeric serum protein assembled from products of three different genes. Biochemistry 1987;26:5229–5233. [PubMed: 3676249]
12. Lebioda, L.; Sodetz, JM. Complement protein C8. In: Morikis, D.; Lambris, JD., editors. Structural Biology of the Complement System. Boca Raton: CRC Press; 2005. p. 233
13. Hobart MJ, Fernie BA, DiScipio RG. Structure of the human C7 gene and comparison with the C6, C8A, C8B, and C9 genes. J. Immunol 1995;154:5188–5194. [PubMed: 7730625]

14. Plumb, ME.; Sodetz, JM. Proteins of the membrane attack complex. In: Volanakis, JE.; Frank, MM., editors. The Human Complement System in Health and Disease. New York: Marcel Dekker; 1998. p. 119
15. van Dijk, W.; DoCarmo, S.; Rassart, E.; Dahlbäck, B.; Sodetz, JM. The plasma lipocalins α1-acid glycoprotein, apolipoprotein D, apolipoprotein M and complement protein C8γ. In: Åkerström, B.; Borregaard, N.; Flower, D.; Salier, JP., editors. Lipocalins. Landes Bioscience/Eurekah: Georgetown; 2006. p. 140
16. Ponting CP. Chlamydial homologues of the MACPF (MAC/perforin) domain. Curr. Biol 1999;9:R911–R913. [PubMed: 10608922]
17. Pipkin ME, Lieberman J. Delivering the kiss of death: progress on understanding how perforin works. Curr. Opin. Immunol 2007;19:301–308. [PubMed: 17433871]
18. Rosado CJ, Buckle AM, Law RH, Butcher RE, Kan WT, Bird CH, et al. A common fold mediates vertebrate defense and bacterial attack. Science 2007;317:1548–1551. [PubMed: 17717151]
19. Slade DJ, Chiswell B, Sodetz JM. Functional studies of the MACPF domain of human complement protein C8alpha reveal sites for simultaneous binding of C8beta, C8gamma, and C9. Biochemistry 2006;45:5290–5296. [PubMed: 16618117]
20. Hadders MA, Beringer DX, Gros P. Structure of C8alpha-MACPF reveals mechanism of membrane attack in complement immune defense. Science 2007;317:1552–1554. [PubMed: 17872444]
21. Tweten RK. Cholesterol-dependent cytolysins, a family of versatile pore-forming toxins. Infect. Immun 2005;73:6199–6209. [PubMed: 16177291]
22. Krissinel E, Henrick K. Secondary-structure matching (SSM), a new tool for fast protein structure alignment in three dimensions. Acta Crystallogr. D. Biol. Crystallogr 2004;60:2256–2268. [PubMed: 15572779]
23. Polekhina G, Giddings KS, Tweten RK, Parker MW. Insights into the action of the superfamily of cholesterol-dependent cytolysins from studies of intermedilysin. Proc. Natl. Acad. Sci. U.S.A 2005;102:600–605. [PubMed: 15637162]
24. Rossjohn J, Feil SC, McKinstry WJ, Tweten RK, Parker MW. Structure of a cholesterol-binding, thiol-activated cytolysin and a model of its membrane form. Cell 1997;89:685–692. [PubMed: 9182756]
25. Lockert DH, Kaufman KM, Chang CP, Husler T, Sodetz JM, Sims PJ. Identity of the segment of human complement C8 recognized by complement regulatory protein CD59. J. Biol. Chem 1995;270:19723–19728. [PubMed: 7544344]
26. Huang Y, Qiao F, Abagyan R, Hazard S, Tomlinson S. Defining the CD59-C9 binding interaction. J. Biol. Chem 2006;281:27398–27404. [PubMed: 16844690]
27. Ortlund E, Parker CL, Schreck SF, Ginell S, Minor W, Sodetz JM, et al. Crystal structure of human complement protein C8gamma at 1.2 Å resolution reveals a lipocalin fold and a distinct ligand binding site. Biochemistry 2002;41:7030–7037. [PubMed: 12033936]
28. Flower DR, North AC, Sansom CE. The lipocalin protein family: structural and sequence overview. Biochim. Biophys. Acta 2000;1482:9–24. [PubMed: 11058743]
29. Plumb ME, Sodetz JM. An indel within the C8 alpha subunit of human complement C8 mediates intracellular binding of C8 gamma and formation of C8 alpha-gamma. Biochemistry 2000;39:13078–13083. [PubMed: 11041874]
30. Lovelace LL, Chiswell B, Slade DJ, Sodetz JM, Lebioda L. Crystal structure of complement protein C8gamma in complex with a peptide containing the C8gamma binding site on C8alpha: Implications for C8gamma ligand binding. Mol. Immunol 2008;45:750–756. [PubMed: 17692377]
31. Ramachandran R, Tweten RK, Johnson AE. Membrane-dependent conformational changes initiate cholesterol-dependent cytolysin oligomerization and intersubunit beta-strand alignment. Nat. Struct. Mol. Biol 2004;11:697–705. [PubMed: 15235590]
32. Schreck SF, Plumb ME, Platteborze PL, Kaufman KM, Michelotti GA, Letson CS, et al. Expression and characterization of recombinant subunits of human complement component C8: further analysis of the function of C8 alpha and C8 gamma. J. Immunol 1998;161:311–318. [PubMed: 9647238]
33. Parker CL, Sodetz JM. Role of the human C8 subunits in complement-mediated bacterial killing: evidence that C8 gamma is not essential. Mol. Immunol 2002;39:453–458. [PubMed: 12413696]

34. Shepard LA, Heuck AP, Hamman BD, Rossjohn J, Parker MW, Ryan KR, et al. Identification of a membrane-spanning domain of the thiol-activated pore-forming toxin Clostridium perfringens perfringolysin O: an alpha-helical to beta-sheet transition identified by fluorescence spectroscopy. Biochemistry 1998;37:14563–14574. [PubMed: 9772185]
35. Shatursky O, Heuck AP, Shepard LA, Rossjohn J, Parker MW, Johnson AE, et al. The mechanism of membrane insertion for a cholesterol-dependent cytolysin: a novel paradigm for pore-forming toxins. Cell 1999;99:293–299. [PubMed: 10555145]
36. Chiswell B, Lovelace LL, Brannen C, Ortlund EA, Lebioda L, Sodetz JM. Structural features of the ligand binding site on human complement protein C8 gamma: A member of the lipocalin family. Biochim. Biophys. Acta 2007;1774:637–644. [PubMed: 17452033]
37. Brickner A, Sodetz JM. Functional domains of the alpha subunit of the eighth component of human complement: identification and characterization of a distinct binding site for the gamma chain. Biochemistry 1985;24:4603–4607. [PubMed: 4063342]
38. Nakamura M, Sekino-Suzuki N, Mitsui K, Ohno-Iwashita Y. Contribution of tryptophan residues to the structural changes in perfringolysin O during interaction with liposomal membranes. J. Biochem 1998;123:1145–1155. [PubMed: 9604004]
39. Kristan K, Podlesek Z, Hojnik V, Gutierrez-Aguirre I, Guncar G, Turk D, et al. Pore formation by equinatoxin, a eukaryotic pore-forming toxin, requires a flexible N-terminal region and a stable beta-sandwich. J. Biol. Chem 2004;279:46509–46517. [PubMed: 15322132]
40. Olson R, Gouaux E. Crystal structure of the Vibrio cholerae cytolysin (VCC) pro-toxin and its assembly into a heptameric transmembrane pore. J. Mol. Biol 2005;350:997–1016. [PubMed: 15978620]
41. Hashimoto H. Recent structural studies of carbohydrate-binding modules. Cell Mol. Life Sci 2006;63:2954–2967. [PubMed: 17131061]
42. Hotze EM, Heuck AP, Czajkowsky DM, Shao Z, Johnson AE, Tweten RK. Monomer-monomer interactions drive the prepore to pore conversion of a beta-barrel-forming cholesterol-dependent cytolysin. J. Biol. Chem 2002;277:11597–11605. [PubMed: 11799121]
43. Brannen CL, Sodetz JM. Incorporation of human complement C8 into the membrane attack complex is mediated by a binding site located within the C8beta MACPF domain. Mol. Immunol 2007;44:960–965. [PubMed: 16624411]
44. Ishino T, Chinzei Y, Yuda M. A Plasmodium sporozoite protein with a membrane attack complex domain is required for breaching the liver sinusoidal cell layer prior to hepatocyte infection. Cell Microbiol 2005;7:199–208. [PubMed: 15659064]
45. Satoh H, Oshiro N, Iwanaga S, Namikoshi M, Nagai H. Characterization of PsTX-60B, a new membrane-attack complex/perforin (MACPF) family toxin, from the venomous sea anemone Phyllodiscus semoni. Toxicon 2007;49:1208–1210. [PubMed: 17368498]
46. Noutoshi Y, Kuromori T, Wada T, Hirayama T, Kamiya A, Imura Y, et al. Loss of Necrotic Spotted Lesions 1 associates with cell death and defense responses in Arabidopsis thaliana. Plant Mol. Biol 2006;62:29–42. [PubMed: 16900325]
47. Voskoboinik I, Smyth MJ, Trapani JA. Perforin-mediated target-cell death and immune homeostasis. Nat. Rev. Immunol 2006;6:940–952. [PubMed: 17124515]
48. Rameix-Welti MA, Regnier CH, Bienaime F, Blouin J, Schifferli J, Fridman WH, et al. Hereditary complement C7 deficiency in nine families: subtotal C7 deficiency revisited. Eur. J. Immunol 2007;37:1377–1385. [PubMed: 17407100]
49. Luft JR, Collins RJ, Fehrman NA, Lauricella AM, Veatch CK, DeTitta GT. A deliberate approach to screening for initial crystallization conditions of biological macromolecules. J. Struct. Biol 2003;142:170–179. [PubMed: 12718929]
50. Otwinowski Z, Minor W. Processing of X-ray diffraction data collected in oscillation mode. Methods Enzymol 1997;276:307–326.
51. Minor W, Cymborowski M, Otwinowski Z, Chruszcz M. HKL-3000: the integration of data reduction and structure solution-from diffraction images to an initial model in minutes. Acta Crystallogr. D. Biol. Crystallogr 2006;62:859–866. [PubMed: 16855301]
52. Schneider TR, Sheldrick GM. Substructure solution with SHELXD. Acta Crystallogr. D. Biol. Crystallogr 2002;58:1772–1779. [PubMed: 12351820]

53. Sheldrick GM. Macromolecular phasing with SHELXE. Z. Kristallogr 2002;217:644–650.
54. Otwinowski, Z. CCP4. Warrington, UK: SERC Daresbury Laboratory; 1991. MLPHARE.
55. Cowtan K. DM: an automated procedure for phase improvement by density modification. Joint CCP4 and ESF-EACBM Newsletter on Protein Crystallography 1994;31:34–38.
56. Jones TA, Zou JY, Cowan SW, Kjeldgaard M. Improved methods for building protein models in electron density maps and the location of errors in these models. Acta Crystallogr. A 1991;47(Pt 2): 110–119. [PubMed: 2025413]
57. Emsley P, Cowtan K. Coot: model-building tools for molecular graphics. Acta Crystallogr. D. Biol. Crystallogr 2004;60:2126–2132. [PubMed: 15572765]
58. Murshudov GN, Vagin AA, Dodson EJ. Refinement of macromolecular structures by the maximum-likelihood method. Acta Crystallogr. D. Biol. Crystallogr 1997;53:240–255. [PubMed: 15299926]
59. Perrakis A, Morris R, Lamzin VS. Automated protein model building combined with iterative structure refinement. Nat. Struct. Biol 1999;6:458–463. [PubMed: 10331874]
60. Terwilliger TC. Automated structure solution, density modification and model building. Acta Crystallogr. D. Biol. Crystallogr 2002;58:1937–1940. [PubMed: 12393925]
61. Holm L, Park J. DaliLite workbench for protein structure comparison. Bioinformatics 2000;16:566–567. [PubMed: 10980157]
62. Kraulis PJ. MOLSCRIPT: a program to produce both detailed and schematic plots of protein structures. J. Appl. Crystallogr 1991;24:946–950.
63. Merritt EA, Bacon DJ. Raster3D: photorealistic molecular graphics. Methods Enzymol 1997;277:505–524. [PubMed: 18488322]
64. DeLano, WL. The PyMOL Molecular Graphics System. San Carlos, CA, USA: DeLano Scientific; 2002. http://www.pymol.org.

Abbreviations used

MAC, membrane attack complex; MACPF, membrane attack complex/perforin; C8α-MACPF, recombinant human C8α MACPF domain produced independently of C8γ; αMACPF-γ, recombinant disulfide-linked dimer of the human C8α MACPF domain and C8γ; αMACPF, the MACPF portion of αMACPF-γ; CDC, cholesteroldependent cytolysin; CDC, cholesterol-dependent cytolysin; TMH, transmembrane β-hairpin; ILY, intermedilysin; PFO, perfringolysin O; SSM, Secondary Structure Matching software.

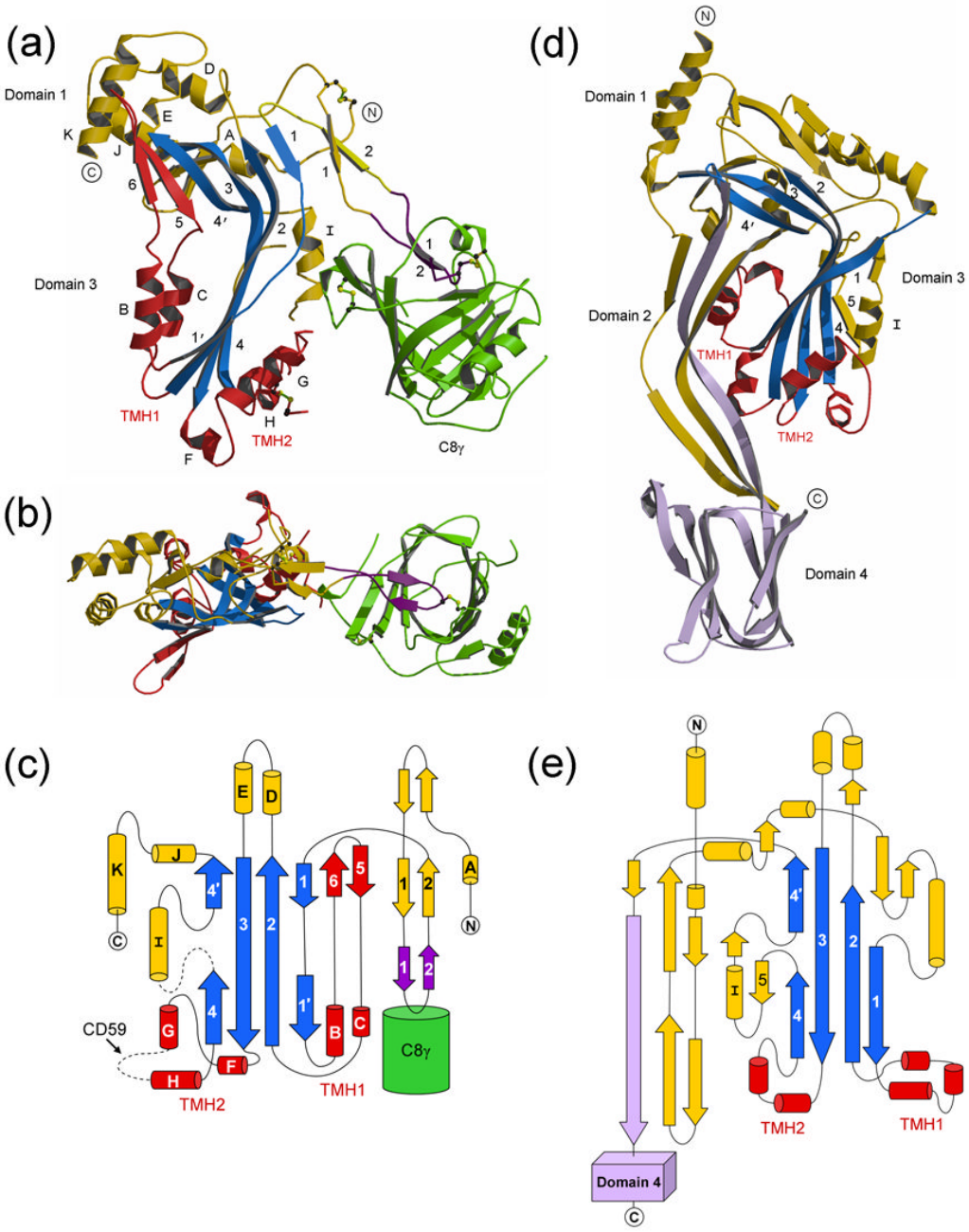

Figure 1.

Structure of αMACPF-γ. a) Ribbon representation of αMACPF-γ. Regions corresponding to domains 1 and 3 and the TMH segments in ILY are labeled as such. C8γ is green, the core β-sheet is blue, TMH segments are red, and the C8α indel is purple. Other structural elements are in gold. Disulfide bonds are atom color. The N- and C-termini of αMACPF are labeled. α-helices are lettered from N- to C-terminus and β-strands within each β-sheet are numbered. β-strands in TMH1 are continuous with core β-sheet strands 1–4 and are numbered 5 and 6. b) Top view of αMACPF-γ. Same coloring as in (a) but the molecule is rotated 90°. c) Topology map of αMACPF-γ secondary structure. Dashed lines are disordered segments. Location of the CD59 binding site is indicated. d) Ribbon representation of ILY (PDB code: **1S3R**).

Domains are labeled as described in the text. The core β-sheet and TMH1 and TMH2 segments are colored as in αMACPF-γ. Strand 5 is a continuation of core β-sheet strands 1–4 and is numbered accordingly. e) Topology map of ILY secondary structure.

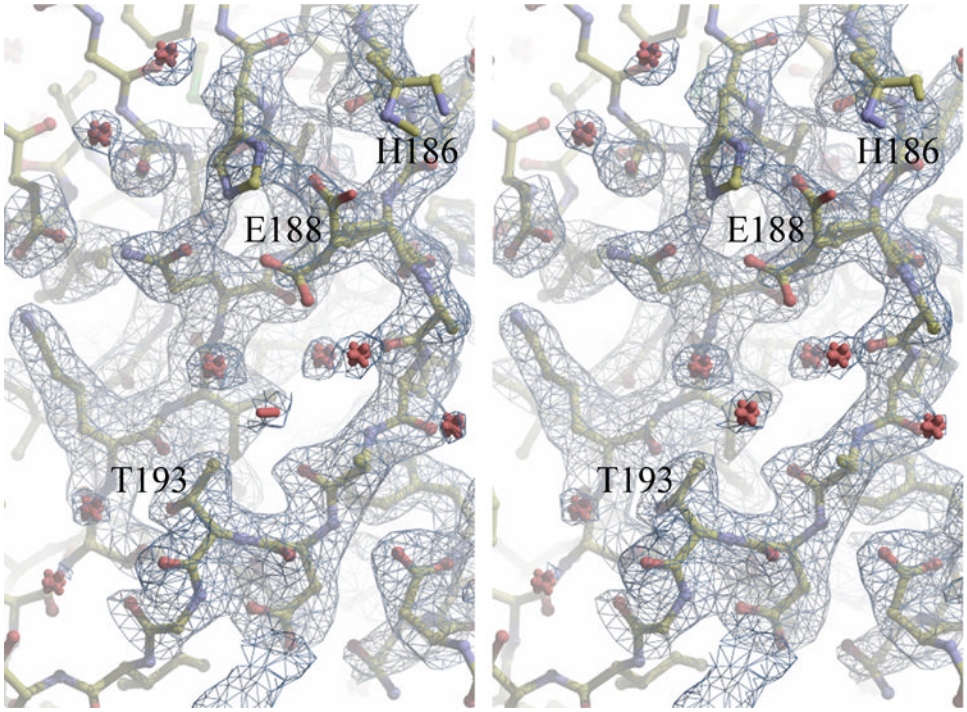

Figure 2.

Stereoview of electron density within the core β-sheet of αMACPF-γ. Electron density (2Fo-Fc coefficients; 1σ contouring level) is from a segment between β-strands 1 and 1' (H186 through T193) and a segment in β-strand 2 (K265 through Q267) in αMACPF. This region lacks the typical hydrogen bonding pattern between strands of a β-sheet as a water molecule bridges the two strands and mediates their interaction. Quality of the density is reflected by the ability to distinguish between two conformations for E188. Figure was generated using COOT.

Figure 3.

Superposition of C8γ structures. The Cα backbone of C8γ from αMACPF-γ (green) is superimposed on the structure of C8γ in complex with the C8α indel peptide (purple) (PDB code: **2QOS**)[7]. The indel peptide is colored red. Four loops surrounding the C8γ calyx entrance are numbered as they occur in the primary structure. In αMACPF-γ, loop 1 in C8γ is moved 10 Å closer to the C8α indel segment. Loops 3, 5, and 7 are also closer by 2, 3.5 and 1 Å, respectively.

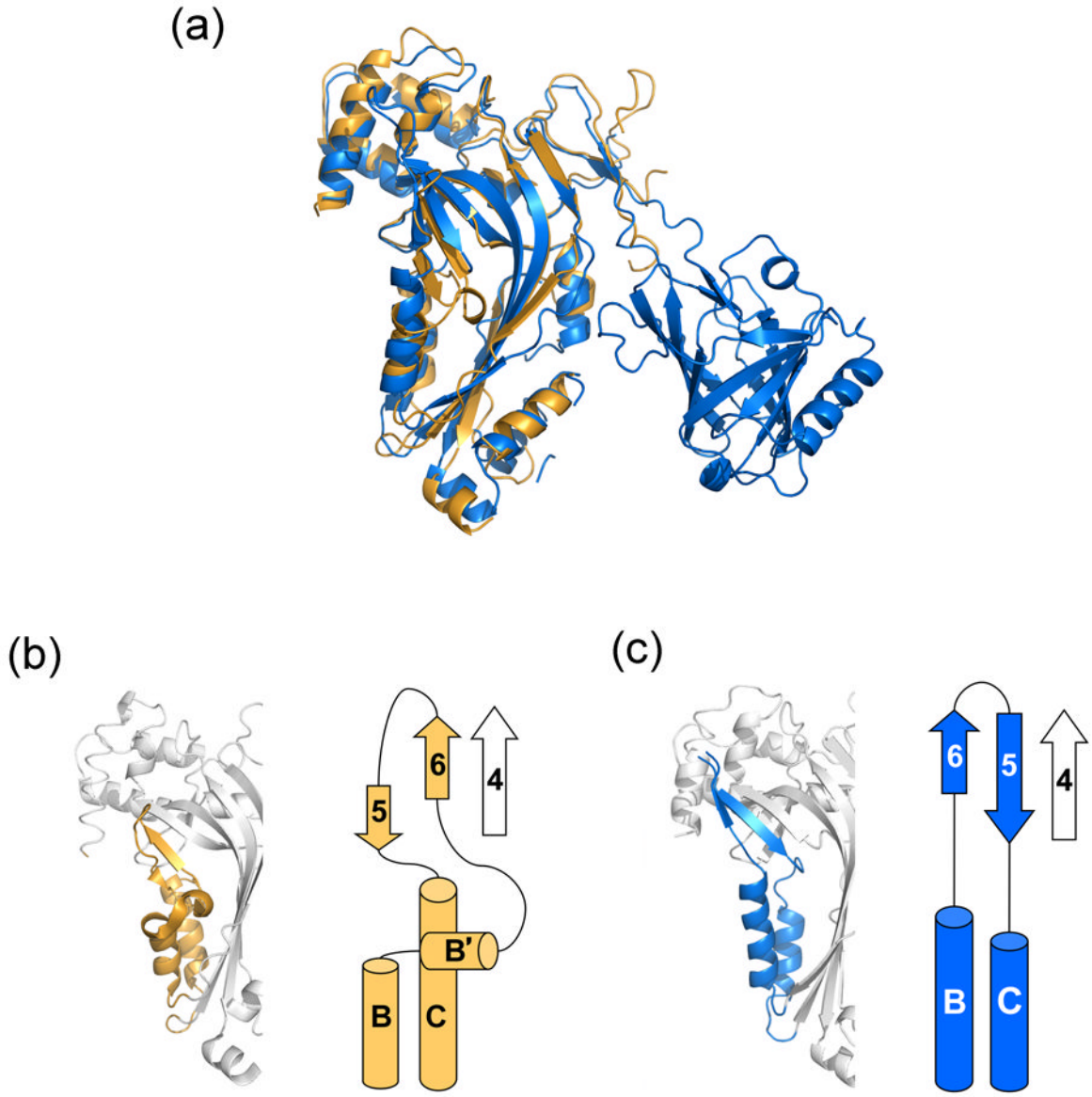

Figure 4.
Structural comparison of C8α-MACPF and αMACPF-γ. a) Superposition of the C8α-MACPF structure (PDB code: **2QQH**) in gold on the αMACPF-γ structure in blue. b) TMH1 region of C8α-MACPF and a corresponding topology diagram. c) The same region in αMACPF-γ.

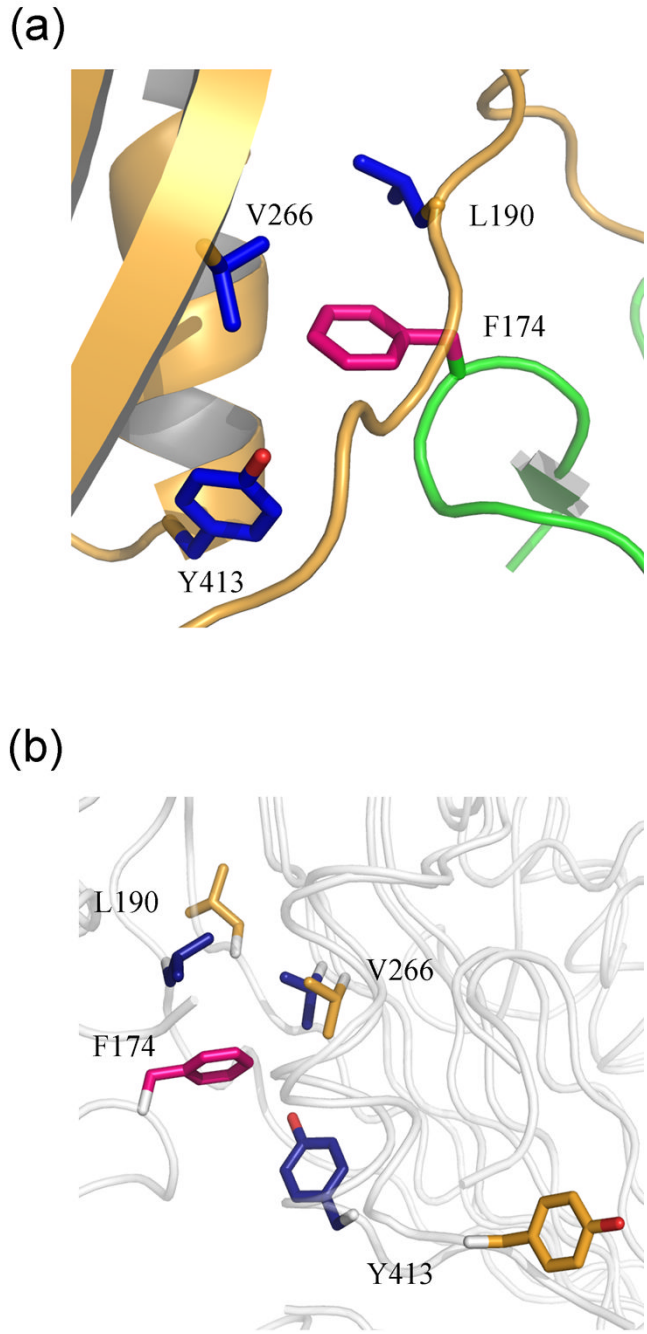

Figure 5.
Contact between C8γ and the αMACPF hydrophobic pocket. a) Interaction between F174 of C8γ (pink) and the hydrophobic pocket created by αMACPF residues L190, V266 and Y413 (in blue). b) Superposition of C8α-MACPF and αMACPF-γ showing conformational changes induced by C8γ. C8α-MACPF sidechains are in orange; αMACPF are in blue.

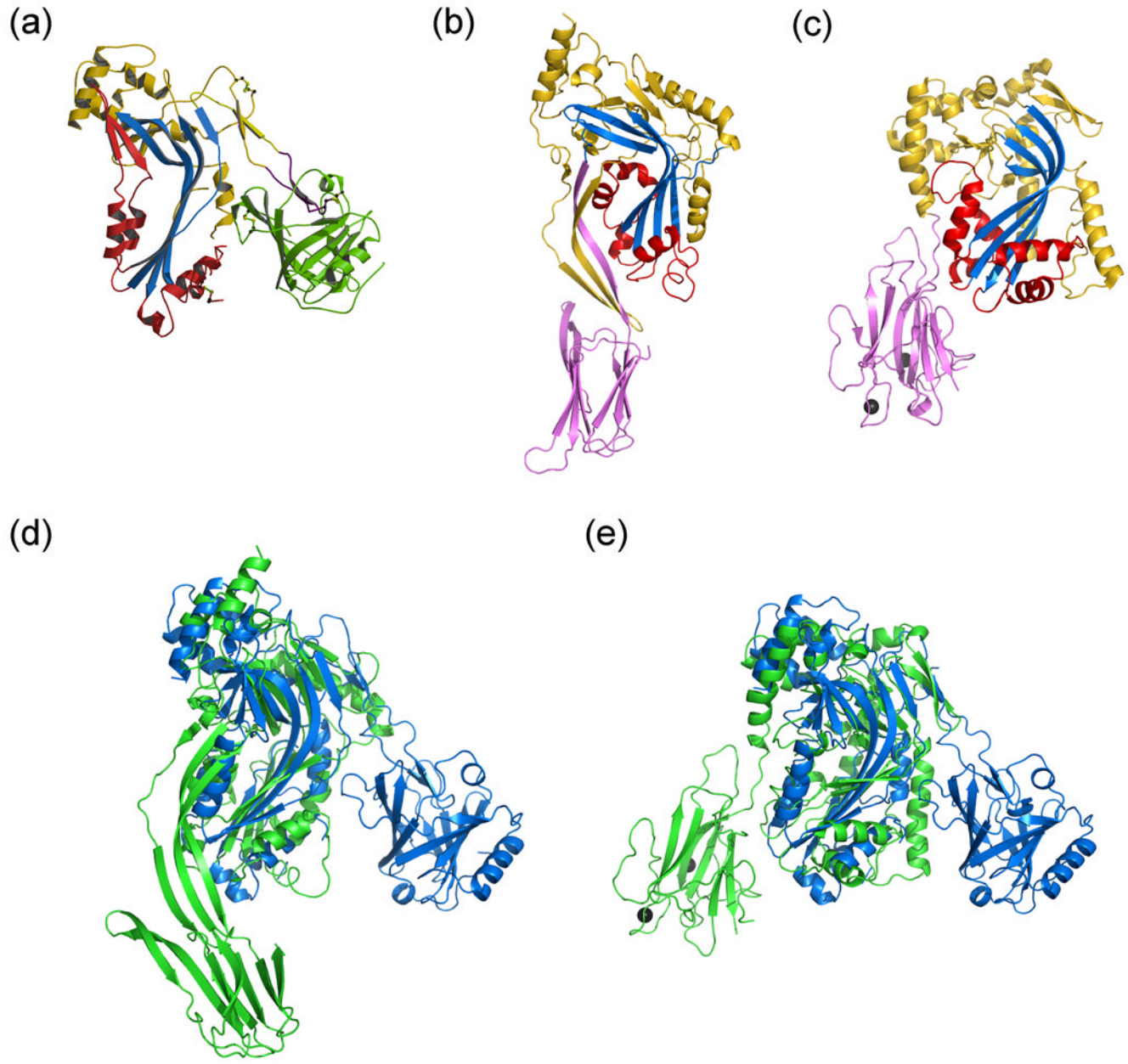

Figure 6.
Comparison of αMACPF-γ, ILY and Plu-MACPF structures. a) αMACPF-γ. b) ILY. c) Plu-MACPF with calcium ions shown in gray (PDB code: **2QP2**). The β-prism domain is purple. d) Superposition of αMACPF-γ (blue) and ILY (green). e) Superposition of αMACPF-γ (blue) and Plu-MACPF (green).

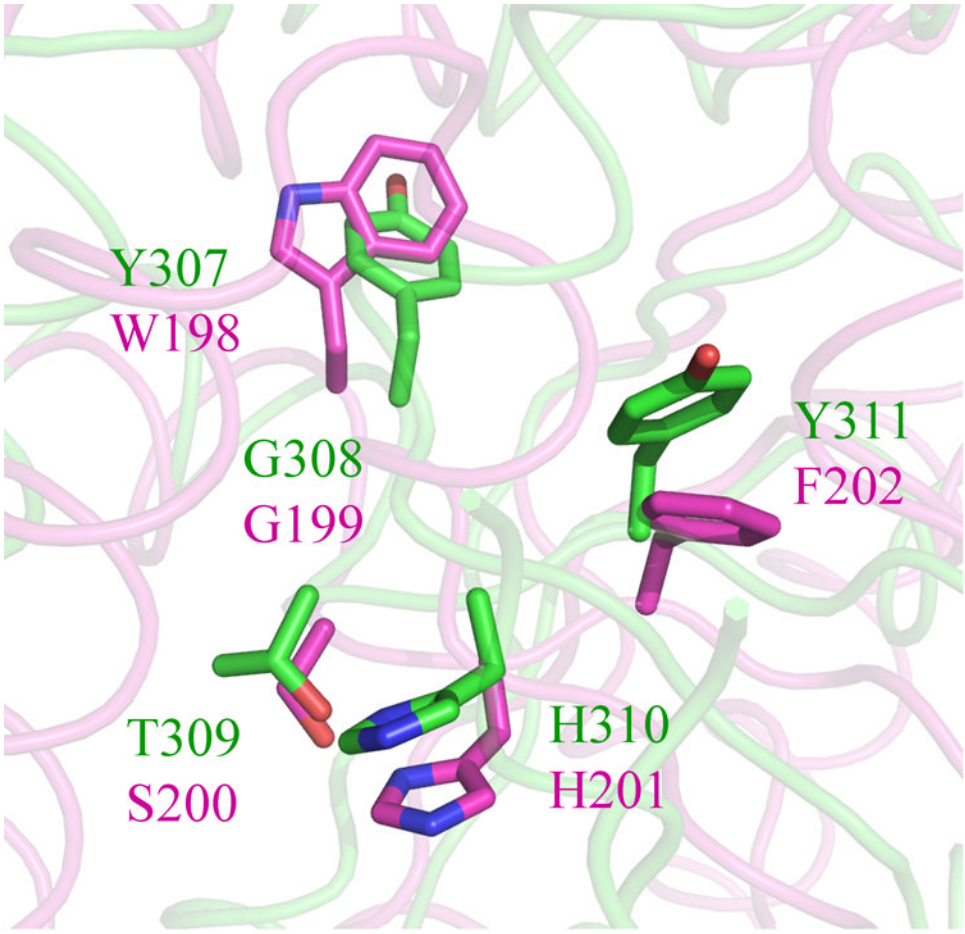

Figure 7.

Y/W-G-S/T-H-F/Y-X_6-G-G motif in αMACPF-γ and Plu-MACPF. Detailed view of the first five residues of the motif in αMACPF-γ superimposed on Plu-MACPF. αMACPF sidechains are in green and Plu-MACPF sidechains are in pink. Not shown are the two glycines at the end of the motif which extend into β-strand 3 of each protein and are also structurally conserved.

Figure 8.

Comparison of MAC protein TMH sequences. Full-length sequence alignments of the MAC family proteins were used to identify segments corresponding to TMH1 and TMH2 sequences in αMACPF. Hydrophobic residues are yellow, polar are green, and charged are red. The conserved intrachain disulfide bond in TMH2 is depicted by a dotted bracket. Secondary structure assignments correspond to those for αMACPF in Figure 1. Also shown are TMH segments in PFO and ILY that are known to interact with membranes.

Table 1

Data collection, phasing, and refinement statistics.

		SeMet αMACPF-γ	αMACPF-γ
Space group		$P2_12_12$	$P2_12_12$
Unit cell		a=95.4Å b=124.3Å c=50.6Å α=β=γ=90°	a=96.6Å b=126.1Å c=51.9Å α=β=γ=90
Data collection			
Structure solution protocol		SAD	MR
Wavelength (Å)		0.9794	0.9565
Resolution (Å)		50.0-2.3	50.0-2.15
Highest resolution shell (Å)		2.32-2.30Å	2.21-2.15
Unique reflections		25296	30735
Redundancy		4.9 (2.2)	4.0 (3.0)
Completeness (%)		93.5 (53.1)	91.9 (77.1)
I/σ(I)		13.9 (1.1)	17.2 (2.4)
R_{merge} (%)		12.7 (58.7)	4.6 (33.4)
SAD analysis			
No. of Se sites located/theoretical		11/13	NA
$FOM_{MLPHARE}$		0.23	NA
FOM_{DM}		0.73	NA
Refinement			
Resolution range (Å)		50.0-2.15	
No. protein atoms/AU		3916	
No. waters/AU		163	
R/R_{free} (%)		20.8/26.1 (30.0/42.3)	
Mean B-factor ($Å^2$)	overall	45.7	
	Protein chain A	53.0	
	Protein chain C	43.7	
	Water molecules	51.5	
RMSD bond length (Å)		0.008	
RMSD angles (°)		1.2	
Ramachandran favored (%)		91.6	
Ramachandran allowed (%)		8.2	
Ramachandran generously allowed (%)		0.2	

Values in parentheses correspond to the highest resolution shell

NA - not applicable

AU – asymmetric part of the unit cell